

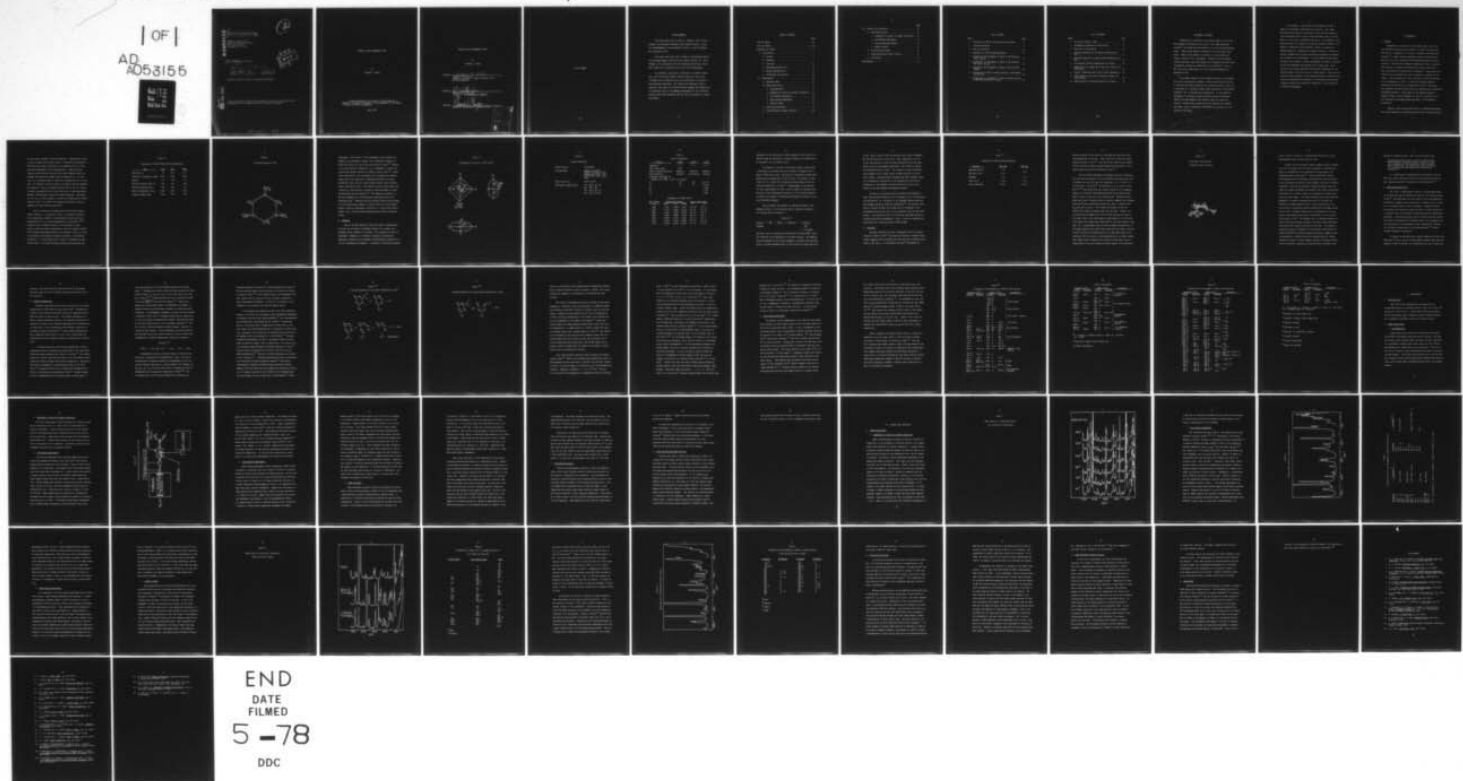
AD-A053 155 DELAWARE UNIV NEWARK DEPT OF CHEMISTRY  
STUDIES OF THE POLYMORPHS OF RDX. (U)  
JUN 78 S T SERGIO

F/G 19/1

UNCLASSIFIED

NL

| OF |  
AD  
A053155  
REF ID: A6274



END

DATE

FILMED

5 -78

DDC

ADA053155

6  
STUDIES OF THE POLYMORPHS OF RDX.

2

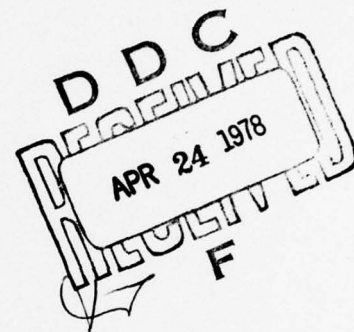
Stephen T. Sergio, CPT  
HQDA, MILPERCEN (DAPC-OPP-E)  
200 Stovall Street  
Alexandria, VA 22332

9 Final Report 12 April 1978

10 Stephen T. Sergio

11 Jun 78

12 70p



Approved for public release; distribution unlimited.

DDC FILE COPY

A thesis submitted to University of Delaware in partial fulfillment of the requirements for the degree of Master of Science in Chemistry.

400 647 70B

STUDIES OF THE POLYMORPHS OF RDX

by

Stephen T. Sergio

A thesis submitted to the Faculty of the University of  
Delaware in partial fulfillment of the requirements for the degree  
of Master of Science in Chemistry.

June, 1978

STUDIES OF THE POLYMORPHS OF RDX

by

Stephen T. Sergio

Approved:

Thomas B. Brill

Thomas B. Brill, Ph.D.

Professor in charge of thesis on behalf of the  
Advisory Committee

Approved:

D. Wetlaufer

Donald B. Wetlaufer, Ph.D.

Chairman of the Department of Chemistry

Approved:

Gerard J. Manjane

University Coordinator of Graduate Studies

ACCESS	REF	STUDY	COLLECTION
NTIS	REF	STUDY	COLLECTION
DOC	REF	STUDY	COLLECTION
ANNOUNCED	REF	STUDY	COLLECTION
JUSTIFICATION	REF	STUDY	COLLECTION
IV			
DISTRIBUTION/AVAILABILITY NOTES			
1. ANALYST	2. APPROVING	3. CIAL	
<b>A</b>			

TO MY PARENTS

#### ACKNOWLEDGMENTS

The author would like to thank Dr. Thomas B. Brill for his guidance and assistance throughout this research project. Grateful acknowledgment is also extended to the U.S. Army for sending me to graduate school.

The author would also like to thank Dr. Suryanarayana Bulusa for providing samples of RDX for this research project, Dr. Peter Leavens for his assistance with the polarizing microscope, and Mr. Neil Cooper for his assistance with the X-ray diffractometer.

My co-workers, Doug Miller, Frank Goetz, Al Landers, Randy Bull, and Geoff Woolery deserve special thanks for their close friendship and for making my stay at the University of Delaware a very enjoyable experience. The author would especially like to thank Mr. Frank Goetz for his many helpful comments and suggestions, the excellent staff at the Chemistry Department for the invaluable services which they performed, and Mrs. Mary Ann Gregson for typing this thesis.

TABLE OF CONTENTS

	Page
List of Tables. . . . .	vii
List of Figures . . . . .	viii
Statement of Problem. . . . .	1
I. Introduction. . . . .	3
A. General . . . . .	3
B. Synthesis . . . . .	7
C. Structure . . . . .	12
D. NMR/Conformational Data . . . . .	17
E. Thermal Decomposition . . . . .	18
F. Vibrational Spectroscopy. . . . .	25
II. Experimental. . . . .	31
A. Materials Used. . . . .	31
B. Raman Spectroscopy. . . . .	31
1. Instrumentation . . . . .	31
2. Dependence of Spectra on Sample Orientation .	32
3. Slow Heating Experiments. . . . .	32
4. Rapid Heating Experiments . . . . .	34
5. $\beta$ -RDX in Thymol . . . . .	35
C. Polarizing Microscope . . . . .	37
D. X-Ray Diffraction Powder Patterns . . . . .	38

	Page
III. Results and Discussion. . . . .	40
A. Raman Spectroscopy. . . . .	40
1. Dependence of Spectra on Sample Orientation .	40
2. Slow Heating Experiments. . . . .	43
3. Rapid Heating Experiments . . . . .	46
4. $\beta$ -RDX in Thymol . . . . .	47
B. Polarizing Microscope . . . . .	54
C. X-Ray Diffraction Powder Patterns . . . . .	56
D. Conclusions . . . . .	57
Bibliography. . . . .	59

### LIST OF TABLES

Table	Page
1 Properties of RDX and Other Military Explosives . . . . .	5
2 Crystal Morphology. . . . .	9
3 Optical Properties. . . . .	10
4 Reactants for RDX and HMX Manufacture . . . . .	13
5 Frequencies and Assignment of Bands in RDX Spectrum (Iqbal, <u>et al.</u> ) . . . . .	27
6 Frequencies and Assignment of Bands in RDX Spectrum (Rey-Lafon, <u>et al.</u> ) . . . . .	29
7 Frequencies and Assignment of Bands in RDX Spectrum (Sergio). . . . .	45
8 Frequencies of Bands in Raman Spectrum of Pure Thymol and Pure RDX. . . . .	50
9 Frequencies and Assignment of Bands in Raman Spectrum of RDX Recrystallized in Thymol . . . . .	53

LIST OF FIGURES

Figure	Page
1 Structural Formula of RDX. . . . .	6
2 Orthographic Projection of RDX Crystal . . . . .	8
3 Side View of RDX Molecule. . . . .	15
4 Proposed Mechanism for Gas Phase Decomposition of RDX. . . . .	21
5 Proposed Mechanism for Liquid Phase Decomposition of RDX. . . . .	22
6 Slow Heating Variable Temperature Cell Design. . . .	33
7 Raman Spectra of Single RDX Crystal as a Function of Orientation. . . . .	41
8 Partial Raman Spectrum of RDX at Room Temperature .	44
9 Raman Spectra of Pure RDX, Crystalline Thymol and Liquid Thymol. . . . .	48
10 Raman Spectrum of Recrystallized RDX in Thymol . . .	52

#### STATEMENT OF PROBLEM

Hexahydro-1,3,5-trinitro-1,3,5-triazine (RDX) is one of the most energetic explosives in use today.<sup>1</sup> Hot stage microscope studies<sup>2,3</sup> have shown that RDX exists in two solid-state polymorphic forms.  $\alpha$ -RDX [called RDX(I) by McCrone] is the only stable polymorph.  $\beta$ -RDX [called RDX(II) by McCrone] is very unstable and rapidly converts to the  $\alpha$ -polymorph. Studies of the  $\beta$ -polymorph would be important since the presence of an unstable polymorph could considerably increase the sensitivity of an explosive.<sup>4</sup> Also,  $\beta$ -RDX could play an important role in the thermal decomposition mechanism of RDX.

The primary purpose of this research has been to investigate the lattice and molecular dynamics of RDX by observing the effects of both slow and rapid heating on the vibrational modes of RDX, and to determine if a thermally induced phase transition to the unstable polymorph can be observed spectroscopically. A laser Raman investigation of octahydro-1,3,5,7-tetranitro-1,3,5,7-tetrazocine (HMX),<sup>5</sup> the eight-membered ring analog of RDX, has shown that thermally induced phase transitions can be observed and recorded with major, easily recognizable differences in the spectra of the different polymorphs.

In an attempt to characterize the  $\beta$ -polymorph of RDX, a number of instrumental techniques were utilized. Laser Raman spectroscopy was used as an analytical probe since the change in ring conformation and/or crystal lattice packing, which one would expect to occur with a transition from the  $\alpha$ - to  $\beta$ -polymorph, would manifest itself by a change in the spectra through a change in the number of vibrational bands observed, a shift in frequency of selected modes or a combination of these two effects. Analysis of spectral changes would provide qualitative information concerning the structure of the  $\beta$ -polymorph. An X-ray powder diffractometer was used in an attempt to verify the presence of  $\beta$ -RDX in a mixture of the two polymorphs when prepared from a thymol melt. Also, analysis of the powder patterns would provide information on the size and shape of the unit cell in a  $\beta$ -RDX crystal. Since the only analytical data available for the characterization of  $\beta$ -RDX are its optical crystallographic properties,<sup>2</sup> a polarizing microscope was utilized to verify the presence of  $\beta$ -RDX prior to the initiation of selected experiments.

## I. INTRODUCTION

### A. General

Hexahydro-1,3,5-trinitro-1,3,5-triazine (RDX), one of the most energetic explosives in use today, is a major military explosive used as a component in a variety of explosive and propellant mixtures. It gained military importance during the Second World War due to its lower sensitivity than PETN (pentaerythritol tetranitrate).<sup>6</sup> RDX was first prepared by Henning in 1899, by reacting the dinitrate of hexamine (hexamethylenetetramine) with nitric acid, and patented for possible use in medicine.<sup>7</sup> Henning gave few details for his synthesis and did not propose a structure for the product. Herz proposed the correct structure for RDX and patented it as an explosive in 1920.<sup>8</sup> In 1925 Hale reported improved directions and details for the preparation of RDX.<sup>9</sup> The symbol RDX originated in Great Britain and is the abbreviation for Research Department Explosive. Other names for the compound included: hexogen (Germany, France, Belgium), T4 (Italy), cyclonite (U.S.A.) and frequently cyclotrimethylenetrinitramine in the chemical literature.<sup>9</sup>

Mixtures of RDX and wax, which acts as a desensitizing agent, are called Composition-A explosives and are used in artillery shells

and as booster chargers in various munitions. Composition-B, which is used in bombs and artillery shells, is prepared by adding RDX to TNT (trinitrotoluene) resulting in an increased velocity of fragments and enhancement of the blasting effect. When mixed with special plasticizers and solvents, RDX yields numerous plastic explosives and demolition charges such as Composition-C. A 9 inch drop of a 2 kilogram weight is required to detonate RDX in the drop test. To detonate 0.4 grams of RDX, 0.17 grams of mercury fulminate are required. Using the standard friction test of the U.S. Bureau of Mines, striking RDX with a fiber shoe fails to cause detonation, whereas, striking with a steel shoe causes detonation. RDX fumes off in 5 sec. at 290°C, however, it does not detonate even at 360°C.<sup>7</sup> Listed in Table 1 are some of the explosive properties of RDX as compared with other military explosives.

RDX is a monocyclic nitramine with the structural formula shown in Figure 1. It exists as a white or colorless crystalline solid (depending on method of crystallization) which melts with decomposition but not violent decomposition, at 204-205°C.<sup>2,6,10</sup> Solubility data on RDX has shown it to be insoluble in water, alcohol, ether and carbon tetrachloride, only very slightly soluble in hot benzene, moderately soluble in hot acetone (1 part in 8) and very soluble in hot aniline and phenol from which it crystallizes as needles.<sup>7</sup> It crystallizes from a variety of solvents into many crystal habits. Hot stage microscope studies have shown that two

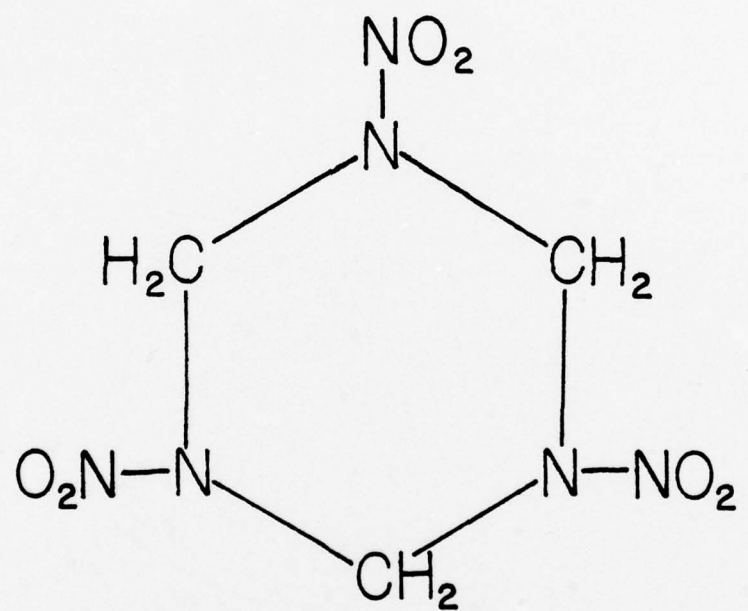
Table 1<sup>9</sup>

## Properties of RDX and Other Military Explosives

<u>Test</u>	<u>RDX</u>	<u>TNT</u>	<u>PETN</u>
Sand test, g	59	43.6	61.2
Velocity of detonation, m/sec	8350	7440	8300
Density	1.7	1.61	1.7
Trauzl lead block test, mL	500	325	500
Ballistic pendulum test	150	110	145
Heat of detonation, cal/g	1300	1065	1385
Volume of gases, mL/g	908	670	790

Figure 1

Structural Formula of RDX



polymorphs,  $\alpha$  and  $\beta$  exist.<sup>3</sup> The  $\alpha$ -polymorph is very stable both chemically and thermally, however, the  $\beta$ -polymorph is highly unstable and exists for only a very short period of time.<sup>2,3</sup> Because of its great physical instability, it is impossible to obtain and preserve well-formed crystals of  $\beta$ -RDX on a macro scale.<sup>2,3</sup> Microscopic quantities of the  $\beta$ -polymorph can be prepared and observed using a micro hot stage with a polarizing microscope, by supersaturating a small drop of a high boiling solvent, such as molten thymol, with RDX at 150°C. The solution is then cooled quickly and a mixture of fine dendritic crystals of  $\beta$ -RDX and plates of  $\alpha$ -RDX recrystallize from the solution.<sup>2,3</sup> The dendritic crystals of  $\beta$ -RDX soon disappear by a solution-phase transformation as the  $\alpha$ -polymorph grows.  $\beta$ -RDX has also been observed during fusion studies on a microscope slide, however, it exists only for a few seconds.<sup>2</sup> Figure 2 shows an orthographic projection of a typical RDX crystal. Tables 2 and 3 list the crystal morphology and optical properties of RDX.

#### B. Synthesis

Most of the RDX produced in the world today is manufactured by either the nitrolysis of hexamine (German S.H. process), the Bachmann process (German K.A. process), or a variation of these two processes.<sup>9</sup> Hexamine is a colorless, odorless and practically tasteless crystalline solid prepared by evaporating an aqueous solution of formaldehyde and ammonia. In addition to being the principle

Figure 2<sup>2</sup>

Orthographic Projection of RDX Crystal

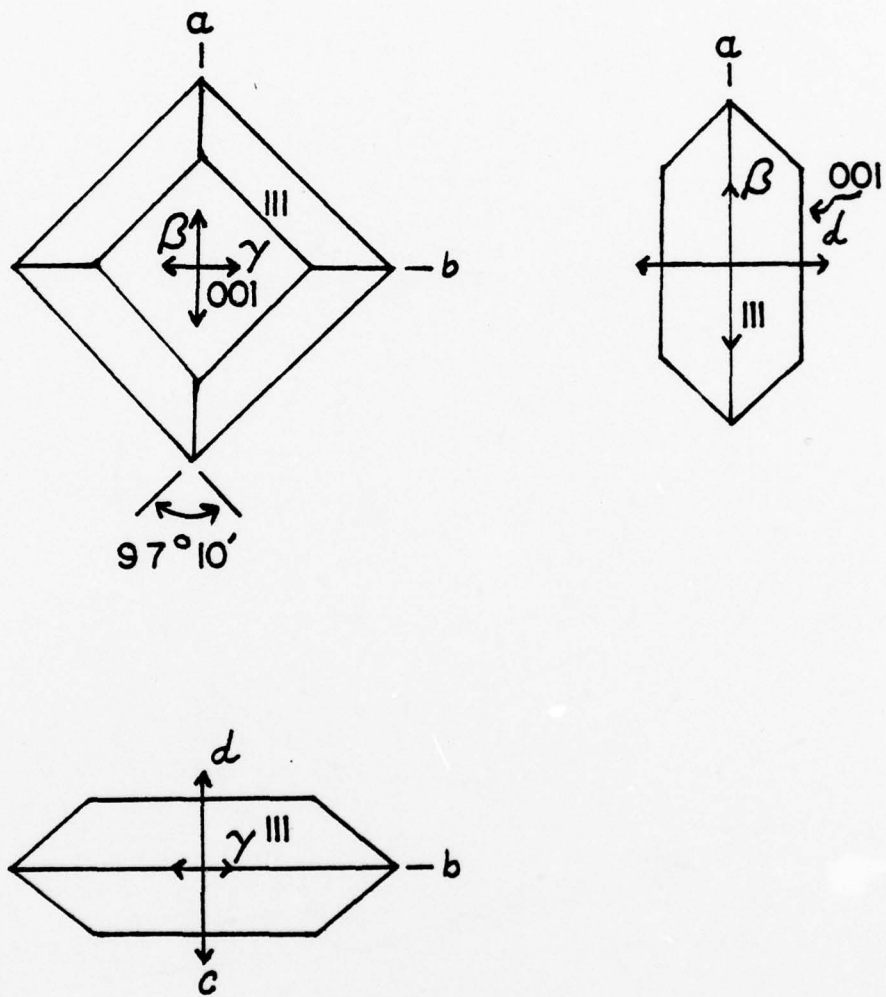


Table 2<sup>2</sup>

## Crystal Morphology

Crystal System	Orthorhombic
Form and Habit	Depends on solvent, usually flattened on 001 showing the forms: {110}, {120}, {101}, {011}, and {111}
Axial ratio a:b:c	0.881:1:0.813
Interfacial angles (polar)	$110 \wedge \bar{1}\bar{1}0 = 82^\circ 50'$ $120 \wedge \bar{1}20 = 59^\circ$ $101 \wedge \bar{1}01 = 85^\circ 30'$ $011 \wedge \bar{0}11 = 78^\circ 20'$

Table 3

## Optical Properties

Property	$\alpha\text{-RDX}^2$	$\beta\text{-RDX}^2$	$\alpha\text{-RDX}^4$
Dispersion	$r > v$	$v > r$	$r \gg v$
Optic axial plane	100		
Sign of double refraction	negative	positive	negative
Acute bisectrix	centered	off-centered	centered
Molecular refraction (R)			
(5893 $\text{\AA}$ , 25°C) $\sqrt[3]{\alpha\beta\gamma} = 1.592$	41.4 (obsd.)		
2E	92°	113°	87-1/2°
2V	53°	67°	51-1/2°
$\alpha_D$			1.580
$\beta_D$			1.595
$\gamma_D$			1.600

Dispersion of  $\alpha\text{-RDX}$  (20°C)<sup>2</sup>

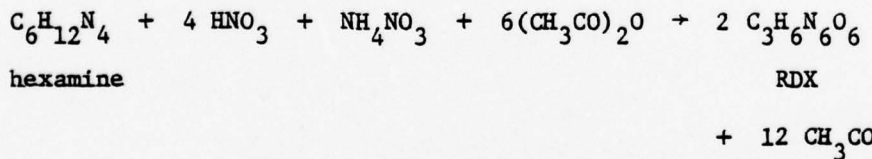
Wave Length of Light, $\text{\AA}$	Refractive Indexes			Optical Axial Angle	
	Alpha	Beta	Gamma	2E	2V
6680	1.5725	1.5906	1.5957	95° 15'	55° 21'
5893	1.5775	1.5966	1.6015	91° 36'	53° 22'
5850	1.5827	1.6031	1.6079	87° 33'	51° 8'
5020	1.5874	1.6084	1.6130	83° 53'	49° 7'
4860	1.5895	1.6113	1.6157	82° 1'	48° 4'
4710	1.5923	1.6145	1.6187	79° 42'	46° 47'
4470	1.5970	1.6205	1.6245	75° 34'	44° 26'

ingredient in the manufacture of RDX, hexamine is also used in industry during the synthesis of several polymers and in medicine as an antiseptic for the urinary tract.<sup>7</sup>

The German S.H. process, as modified by Hale, produces RDX in 68% yield by nitrating one part by weight of hexamine with 11 parts of 100% nitric acid. The mixture is vigorously stirred while maintaining the temperature at 30°C or less. The product is then cooled to 0°C, stirred for an additional twenty minutes then filtered and washed with ice water.<sup>9</sup> Disadvantages of this process are that large amounts of nitric acid are needed for maximum yield and much of the formaldehyde by-product is lost through oxidation by nitric acid instead of combining with ammonia by-product to produce additional hexamine.

The most widely used method for manufacturing RDX is the Bachmann process. In this process, RDX is produced according to the reaction shown in equation 1.

Equation 1<sup>9</sup>



The acetic acid is recovered by distillation from the mother liquor and converted to the anhydride by the Wacker process. The ammonium nitrate combines with by-product fragments, containing the methylene group, to produce hexamine which in turn produces an additional mole

of RDX. Thus, 2 moles of RDX are produced from 1 mole of hexamine. The reaction mixture is run at 75°C. Upon completion of the reaction, the mixture is cooled and RDX precipitates from the supernatant liquor in approximately 80% yield. The product is washed and stabilized with hot water.<sup>9</sup> The reaction is quite exothermic; thus, reagents must be added slowly in small portions to the reaction vessel. Although several theories have been proposed, there is no satisfactory description of the mechanism for the partial degradation of the hexamine ring when reacted with nitric acid, because of the many complex intermediates formed.<sup>9</sup>

Currently in the United States at Holston Army Ammunition Plant, RDX and HMX (octahydro-1,3,5,7-tetranitro-1,3,5,7-tetrazocine) are manufactured by a variation of the Bachmann process using the same reagents except in different proportions.<sup>11</sup> The initial crude product contains 79% RDX, and 6% HMX which is considered a non-detrimental impurity and, thus, is not separated from the final RDX product. The reaction is run at 75°C and the crude RDX obtained is recrystallized from cyclohexanone. Table 4 lists the reactants and proportions for a 100 pound batch of RDX and HMX.

#### C. Structure

Hultgren conducted the first investigation into the crystal structure of RDX in 1936.<sup>12</sup> He found the molecule to possess orthorhombic symmetry with 8 molecules per unit cell and a probable space group of  $V_h^{15}$  (Pbca). In 1959 Harris and Reed<sup>13</sup> determined the

Table 4<sup>11</sup>

## Reactants for RDX and HMX Manufacture

<u>Reactant</u>	<u>RDX, kgs</u>	<u>HMX, kgs</u>
Ammonium Nitrate	7.79	4.98
98% Nitric Acid	6.16	
Hexamine	4.17	7.70
Acetic Acid	6.80	8.15
Acetic Anhydride	20.39	24.46

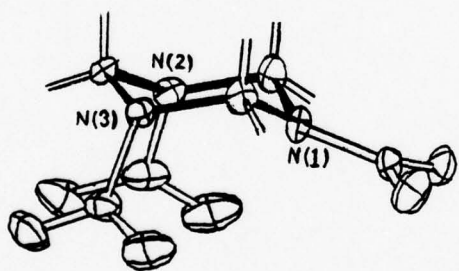
crystal structure of RDX except for hydrogen atom positions using three-dimensional X-ray data. Their X-ray work on RDX was further refined by Filhol in 1970.<sup>14</sup> Choi and Prince reported the complete crystal structure of RDX including hydrogen atom positions in 1972 using single-crystal neutron-diffraction data.<sup>15</sup>

Choi and Prince confirmed the findings of earlier investigators that RDX crystallizes in the orthorhombic space group Pbca with 8 molecules per unit cell and cell dimensions of  $a = 13.182 \text{ \AA}$ ,  $b = 11.574 \text{ \AA}$  and  $c = 10.709 \text{ \AA}$ .<sup>15</sup> The molecule is at a  $C_1$  site of symmetry.<sup>15,16</sup> They showed that the molecule consists of a 6-membered puckered C-N ring with alternating methylene and nitramine groups. Figure 3 shows a side view of the RDX molecule. Methylene carbon atoms were found to possess nearly tetrahedral symmetry and nitramine groups were either essentially planar  $[\text{N}_{(1)}-\text{NO}_2]$  or slightly bent  $[\text{N}_{(2)}-\text{NO}_2 \text{ and } \text{N}_{(3)}-\text{NO}_2]$ . Bond lengths and angles for the two slightly bend axial nitramine groups were the same. However, for the equatorial nitramine group, the N-N bond distance was found to be shorter than in the axial groups by approximately  $0.04 \text{ \AA}$  and the C-N-N angles were larger than those found in the axial groups by more than  $3 \text{ \AA}$ . An approximate plane of mirror symmetry perpendicular to the plane defined by the three carbon atoms was also noted. Choi and Prince<sup>15</sup> postulated the RDX molecule to be semi-rigid based on observations that one proton of each methylene group is always located near oxygen atoms of adjacent nitro groups on both sides, and the oxygen atoms of the nitro groups are bound tightly to the molecular

Figure 3<sup>15</sup>

Side View of RDX Molecule

(Hydrogen atoms not shown)



ring by strong O...H and O...C interactions which tend to cause approximately planar  $C_2N\cdot NO_2$  groups to form.

Insight into the molecular crystal packing of RDX is offered by Stals who proposed that the crystal packing is controlled primarily by intramolecular and intermolecular electrostatic and hydrogen-bonding interactions.<sup>17</sup> Using the VESCF-MO (variable electronegativity self-consistent field-molecular orbital) method, he has calculated the electric dipole moments, molecular ionization potentials, electron bond energies, charge distribution and bond orders for simple nitramines and contended that simple valence bond structures do not readily predict the calculated MO charge distribution and bond orders. He further contended that these calculated parameters for simple nitramines also hold for the axial and equatorial nitramine groups of RDX. Stals proposed that it is electrostatic interactions between intermolecular nitramine groups and not  $CH_2\cdots O$  hydrogen bonding that is responsible for the apparently unfavorable electrostatic conformation of the two axial nitro groups in RDX.<sup>17</sup> He discounts  $CH_2\cdots O$  hydrogen bonding as a major force since hydrogen bonding of the weakly acidic methylene protons has been observed only with strong bases. The packing of equatorial groups is explained by intermolecular interatomic distances and VESCF-MO calculated charge distribution. Based on these two parameters, a definite pairing of opposite-sign net charges between the atoms of nearest neighbor equatorial nitramine groups would be predicted, implying a strong attractive coulombic force

between the nitramine groups. Thus, Stals postulated that,

The favorable electrostatic attractive forces between nearest-neighbor equatorial groups, balanced by repulsive intermolecular axial-equatorial and axial-axial group interactions, are sufficiently large to overcome the intramolecular axial-axial group electrostatic repulsions.<sup>17</sup>

As a rapid means of identification of explosives, such as RDX, X-ray powder diffraction patterns have been recorded and the most intense interplanar d spacings have been tabulated.<sup>2,18</sup>

#### D. NMR/Conformational Data

The <sup>1</sup>H and <sup>13</sup>C NMR chemical shifts of the methylene groups in RDX have been used by Farminer and Webb for the characterization of RDX.<sup>19</sup> One might expect an "AB" pattern for the ring methylene protons due to geminal proton interaction. However, only a singlet at  $\delta$  = 6.09 ppm relative to TMS is observed. Farminer and Webb rationalized this finding as being the result of rapid inversion of a flattened ring, thus rendering the methylene protons magnetically equivalent. Literature articles cited by Farminer and Webb support this theory by proposing the nitramine groups to be conjugated, and the N-NO<sub>2</sub> moiety to be essentially planar, implying sp<sup>2</sup> character for the amino nitrogen atom in the nitramine group.<sup>19</sup> Minimal nitrogen inversion is predicted.

In support of the above work, studies conducted by Filhol and Cherville,<sup>16</sup> using a variety of instrumental methods, have shown the symmetry of RDX in solution to be essentially C<sub>3v</sub> due to rapid ring

inversion, with some distortion associated with the  $\text{NO}_2$  groups.

They also found the cyclic nitrogen atoms to oscillate about their  $\text{sp}^2$  positions.

#### E. Thermal Decomposition

Numerous investigations have been conducted into the thermal decomposition of RDX during the past thirty years. Decomposition studies of this explosive have been conducted at temperatures both above and below its melting point. The thermal decomposition of RDX is a highly exothermic reaction. Heat generated during the decomposition process, which increases exponentially with temperature, is either lost to the surroundings through thermal conduction or accumulates within the explosive.<sup>20</sup> During thermal decomposition, heat accumulates faster than it is lost, thus, accelerating the decomposition reaction leading ultimately to deflagration or detonation.

It has been shown that the initial decomposition of RDX at temperatures below its melting point takes place in the vapor phase producing several products, one of which is a liquid.<sup>21</sup> This liquid, acting as a solvent, then dissolves some of the solid RDX and accelerates the reaction through liquid phase decomposition. RDX has not been found to decompose to any significant extent in the solid phase.<sup>21</sup> Nitrogen has been found to inhibit the decomposition reaction by suppressing the vaporization of RDX.<sup>21</sup> Thermal decomposition at temperatures above the melting point has been shown to

occur simultaneously in both the gaseous phase and the liquid phase.<sup>22</sup> Decomposition products which have been isolated and identified include: N<sub>2</sub>, N<sub>2</sub>O, NO, CO<sub>2</sub>, CO, H<sub>2</sub>O, HCN, CH<sub>2</sub>O, NO<sub>3</sub><sup>-</sup>, NO<sub>2</sub><sup>-</sup>, and a liquid.<sup>21,22</sup> Polymerized HCN and a water insoluble polymer of the type  $\text{N}-\text{CH}_2-\text{CH}_2-\text{N}^+$ <sub>n</sub> have also been observed.<sup>21</sup> Formic acid, ammonia and an equivalent amount of formaldehyde are present in combined form as the yellow-brown, resinous, non-volatile liquid consisting of hydroxymethyl formamide, its dimer and other polymeric material of this type.<sup>21</sup> Nitrogen dioxide has been identified in the early stages of decomposition, however, none has been found in the final product mixture due to secondary reactions.<sup>22</sup> The NO<sub>3</sub><sup>-</sup> and NO<sub>2</sub><sup>-</sup> ions were probably produced through a reaction involving the NO<sub>2</sub> molecule. Another explanation of why NO<sub>2</sub> has not been observed in the final product mixture is that it reacts with formaldehyde at elevated temperatures according to Equation 2.

Equation 2<sup>23</sup>



Decomposition products have been shown to catalyze either positively or negatively the decomposition of RDX. The rate of decomposition is markedly catalyzed by formaldehyde and the non-volatile residue liquid and to a lesser extent by NO, whereas, N<sub>2</sub>, NO<sub>2</sub>, N<sub>2</sub>O, NO, CO<sub>2</sub>, CO and H<sub>2</sub>O were found to suppress the rate of decomposition by retarding the vaporization of RDX.<sup>21,24</sup> The catalyzing effect of NO has been explained as resulting from

secondary oxidation reactions with other decomposition products.<sup>25</sup>

The non-volatile residue liquid catalyzes the rection by acting as a solvent for RDX.<sup>21,24</sup> The catalytic effect of formaldehye probably results from its reaction with NO<sub>2</sub> as shown in Equation 2, thus, eliminating an inhibitor. It also is a co-reactant in the formation of the catalytic non-volatile residue liquid.

The decomposition mechanism for RDX is not well understood, however, it is known that the gaseous phase decomposition mechanism is different from the liquid phase mechanism.<sup>25</sup> Both intramolecular and intermolecular interactions may be involved. As mentioned earlier, the initial step in decomposition of RDX occurs in the vapor phase. The rate-determining step is believed to involve homolytic cleavage of the N-N bond in the nitramine group since this is the weakest bond in the molecule (D = 66 kcal/mole).<sup>26</sup> Proposed decomposition mechanisms for RDX in the gaseous phase and liquid phase are shown in Figure 4 and 5, respectively. The initial step in the gaseous phase decomposition involves elimination of NO<sub>2</sub>,<sup>22</sup> whereas, CH<sub>2</sub>O is eliminated in the initial step of the liquid phase decomposition.<sup>25</sup> Rational for these mechanisms can be found in the literature.<sup>25</sup> A different mechanism involving an intermolecular interaction has been proposed by Batten.<sup>24</sup> Work done by Suryanarayana, Graybush and Autera using isotopically labeled samples of HMX has shown that the decomposition products N<sub>2</sub>O and N<sub>2</sub> are not formed by rupture of the N-N bond in the nitramine group and the nitrogen atom in NO comes from a ring nitrogen.<sup>27</sup> These

Figure 4<sup>25</sup>

## Proposed Mechanism for Gas Phase Decomposition of RDX

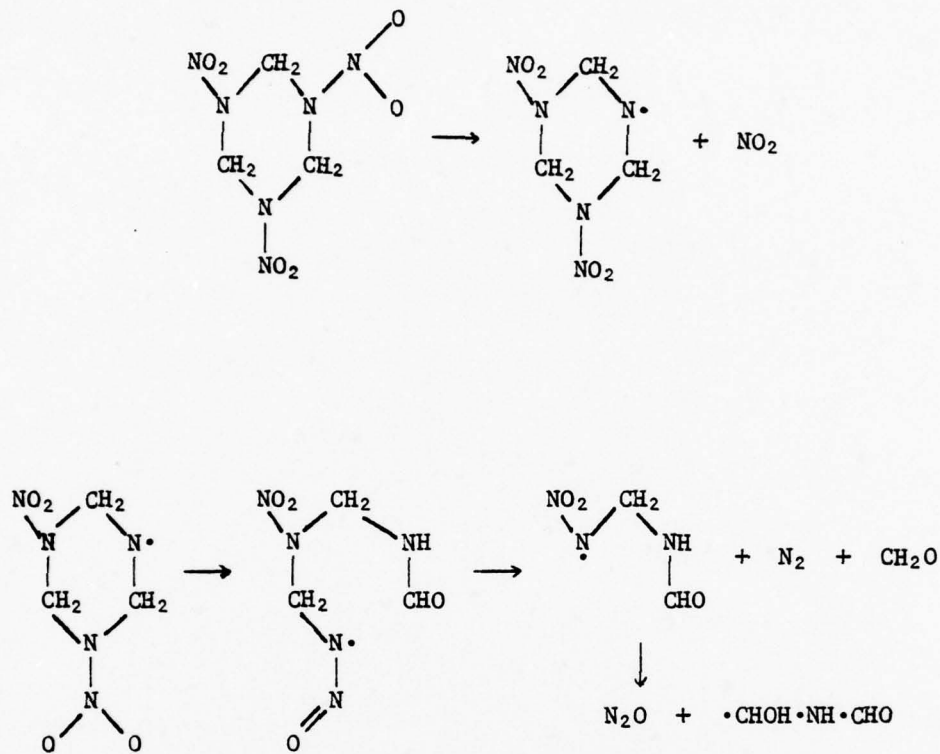
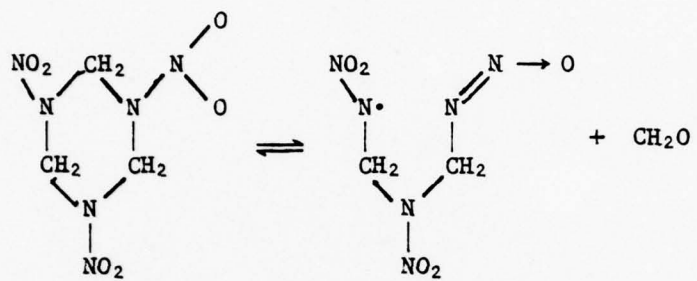


Figure 5<sup>25</sup>

## Proposed Mechanism for Liquid Phase Decomposition of RDX



results are consistent with the gaseous phase decomposition mechanism of Cosgrove and Owen as shown in Figure 4, however, the isotope studies also suggested an intermolecular interaction may have occurred.

The course of decomposition has been followed by monitoring pressure as a function of time, and resulted in a sigmoidal shaped curve showing a continuous increase in pressure until the reaction ceased. Cosgrove and Owen showed that the rate of decomposition of RDX is directly proportional to the volume of the reaction vessel and independent of the weight of the sample.<sup>21</sup> Batten and Murdie showed that sample geometry significantly affects the rate of decomposition. A sample spread in a reaction vessel was found to decompose faster than a sample heaped in a tube.<sup>28</sup> They explained this finding as resulting from the increased surface area of a spread sample which would allow for more rapid diffusion of reaction inhibiting product gases away from the RDX sample and for greater contact of sample with the catalytic non-volatile residue liquid, thus, accelerating the reaction.

First order kinetics have been shown to govern the decomposition of RDX.<sup>29</sup> Kinetic data obtained from pressure-time plots of RDX decomposition have been used to calculate the Arrhenius frequency factor, A, and the energy of activation  $E_a$ , for the decomposition reaction. Robertson calculated:  $A = 3.2 \times 10^{18} \text{ sec}^{-1}$  and  $E_a = 47.5 \text{ kcal mole}^{-1}$  for decomposition at temperatures above the melting

point of RDX.<sup>29</sup> He also determined the half-life of RDX at 213°C to be 410 seconds and at 299°C to be 0.25 seconds. In close agreement with Robertson's kinetic data, Rauch and Fanelli calculated:

$A = 1.7 \times 10^{19} \text{ sec}^{-1}$  and  $E_a = 48.7 \text{ kcal mole}^{-1}$ .<sup>22</sup> These large values for the Arrhenius frequency factor are believed to result from autocatalysis due to self heating and the effect of the non-volatile residue liquid. Batten and Murdie found the decomposition kinetics not to be very temperature sensitive over the range studied (170-198°C).<sup>30</sup> They calculated an  $E_a$  of 63 kcal mole<sup>-1</sup> for a spread sample of RDX and values of 49, 43 and 62 kcal mole<sup>-1</sup> respectively for the induction, acceleration and maximum rate portions of the pressure-time curves for unspread samples.<sup>30</sup> For the spread sample, the  $E_a$  of 63 kcal mole<sup>-1</sup> is approximately equal to the bond dissociation energy of the weakest bond, the N-N nitramine bond (62 kcal mole<sup>-1</sup>).<sup>26</sup> For the heaped sample, the lowering of the activation energy was attributed to the catalytic effect of the decomposition product formaldehyde.<sup>26</sup> As the formaldehyde permeated the heaped sample, the rate of reaction increased and the energy of activation decreased. To test this theory, Batten studied the effect of formaldehyde on spread samples of RDX and found the energy of activation to be lowered from 63 kcal mole<sup>-1</sup> to 44 kcal mole<sup>-1</sup>. Kinetic data have also been obtained using differential thermal analysis (DTA) and differential scanning calorimetry (DSC) methods. Using DTA, Miles calculated:  $A = 6.9 \times 10^{20} \text{ sec}^{-1}$  and  $E_a = 49.5 \text{ kcal mole}^{-1}$  using an unspread sample with heating rates

ranging from  $2.4-30 \text{ K min}^{-1}$ .<sup>20</sup> He observed a decomposition exotherm covering the range 501-528 K. His thermograms showed no evidence of a solid-phase transition. Hall calculated an energy of activation of  $42.5 \text{ kcal mole}^{-1}$  using DSC.<sup>31</sup> At a heating rate of  $8 \text{ K min}^{-1}$ , Hall's thermograms showed a fusion endotherm ( $\Delta H_f = 8.52 \text{ kcal mole}^{-1}$ ) at 478.5 K immediately followed by a decomposition exotherm ( $-\Delta H_d = 136 \text{ kcal mole}^{-1}$ ) covering the range 483-534 K. As with the DTA studies of Miles, no solid-phase transition was observed.<sup>31</sup>

#### F. Vibrational Spectroscopy

Two groups, acting independently, have conducted room temperature infrared and laser Raman studies of both the normal modes and the lattice vibrational modes of RDX. To aid in assignment of the vibrational modes, Iqbal, Suryanarayanan, Bulusa and Autera measured the spectra of two types of  $\text{N}^{15}$  labeled samples;  $\text{N}^{15}$  ring nitrogens and  $\text{N}^{15}$  nitro group nitrogens.<sup>32</sup> They also recorded solution spectra in various solvents. Considerable strain on the RDX ring in the crystalline state was predicted based on abnormally high  $\text{CH}_2$  asymmetric stretch bands. Five bands observed in the region  $50-110 \text{ cm}^{-1}$  were attributed to lattice modes.<sup>32</sup> Comparable results were obtained from infrared and laser Raman studies of RDX conducted by Rey-Lafon, et al. They measured and interpreted solid and solution spectra of both unlabeled and  $\text{N}^{15}$  labeled samples of RDX over the range  $3200-200 \text{ cm}^{-1}$ .<sup>33</sup> Infrared dichroic studies on an oriented polycrystalline film and laser Raman studies of a single crystal

with varied orientation and direction of polarization were also conducted. They showed that in the condensed phase, coupling exists between  $\text{NO}_2$  groups in the different molecules of the unit cell and that in solution, only one rotational isomer exists with the molecule ring possessing  $C_{3v}$  symmetry.<sup>33</sup> In a supplemental study, Rey-Lafon, et al. measured and interpreted the infrared and laser Raman spectra of oriented single crystals of RDX in the region 200-10  $\text{cm}^{-1}$ .<sup>34</sup> They conducted an infrared dichroic study in this region and also showed that strong intermolecular interactions occur between RDX molecules in the unit cell. Tables 5 and 6 list the infrared and laser Raman bands for RDX with their assignments as measured and interpreted by Iqbal, et al. and Rey-Lafon, et al. respectively.

Werbin conducted an infrared study of RDX as a function of temperature over the range -180°C to 220°C and found no marked variations in the position or intensity of bands.<sup>35</sup> Goetz and Brill conducted laser Raman studies of HMX, the eight-membered ring counterpart of RDX, as a function of temperature and observed spectral changes indicating thermally induced phase transitions.<sup>5</sup> A major portion of the work described in this thesis involves similar laser Raman temperature studies of RDX with the goal of spectroscopically observing a thermally induced phase transition of  $\alpha$ -RDX to the unstable  $\beta$ -polymorph.

Table 5<sup>32</sup>

## Frequencies and Assignments of Bands in RDX Spectrum

Infrared (cm <sup>-1</sup> )		Raman (cm <sup>-1</sup> )		Assignments
Solid	Solution	Solid	Solution	
		50.3 <sup>a</sup> s		
		59.2 vs		
		71.5 s		
		85.7 m		
		107 m		
		128 m br		
		148 m br		
		183 w		
225 ms		206 m		
		224 s		
346 s		349 s		
412 m		410 w	410 m	C-N-C bend
460 m		464 m	470 w	
487 m		487 w, br	490 w	
595 m	595 m	590 <sup>b</sup> m	sol. <sup>c</sup> c	NO <sub>2</sub> skeletal
610 m	610 m sh	605 <sup>b</sup> m	sol.	
675 w		671 w	sol.	
740 w sh	740 w	738 w	sol.	
754 m	750 m	758 w	sol.	NO <sub>2</sub> deformation
782 m	794 m	787 w	790 m	
844 m		847 m	845 m	
854 m		854 w sh	850 m sh	
882 m	885 w sh	880 vs	885 ms	Symmetric ring stretch
917 vs		910 m	916 w	
927 vs				
947 s	935 s	940 m	947 w	
1020 m	1015 s	1030 m		
1040 s	1045 m sh		sol.	Ring
1219 m		1217 s	1214 m	
1232 m	1230 m sh	1232 w sh		Ring
1267 s				
1275 s sh	1270 s	1274 s	1268 vs	NO <sub>2</sub> symmetric stretch

Table 5 (continued)

Infrared (cm <sup>-1</sup> )		Raman (cm <sup>-1</sup> )		Assignments
Solid	Solution	Solid	Solution	
1312 m	1320 m	1313 s	1309 m	N-N symmetric stretch
1322 m				
1352 m		1344 w	1339 w	CH <sub>2</sub> skeletal modes
1391 m	1392 m	1382 m sh	1384 m	
1424 m		1389 m		CH <sub>2</sub> skeletal modes
1435 m	1435 m	1427 m sh	1434 m	
1460 m	1460 m	1461 w		NO <sub>2</sub> asymmetric stretch
		1509 w		
1535 ms	1550 m sh	1544 m	1542 m sh	CH <sub>2</sub> symmetric stretch
1576 s		1574 m		
1593 s <sup>b</sup>	1585 s	1577 m sh		CH <sub>2</sub> asymmetric stretch
2950 w	2980 w	1596 m	1582 s	
3006 m		3004 s	2967 s	CH <sub>2</sub> asymmetric stretch
3068 ms		3067 m	3074 m	
3078 s	3080 m	3074 m		

a) s - strong, m - medium strong, w - weak, sh - shoulder,  
br - broad

b) observed in single crystal sample only

c) solvent interference

Table 6<sup>33</sup>

## Frequencies and Assignment of Bands in RDX Spectrum

Infrared (cm <sup>-1</sup> )		Raman (cm <sup>-1</sup> )		Assignment
Solid	Solution	Solid	Solution	
3075 s	3070 w	3075 m	3070 m	$\nu_a$ (CH <sub>2</sub> )
3066 s		3067 m		
3001 m		3001 s		
2948 w	2967 w	2949 s	2970 m	$\nu_s$ (CH <sub>2</sub> )
2922 w				(e)
2855 w				(e)
1598 vs				
1591 vs	1591 vs	1593 w	1581 m	
1573 vs	1580 sh s	1570 w	1575 m	$\nu_a$ (NO <sub>2</sub> ) (d)
1540 s	1555 sh m	1538 w	1550 sh	
1532 s				
1459 s	1455 w	1458 vw	1510 vw	(e)
1434 m	1431 w	1433 w	1450 sh	
1423 m		1422 sh	1432 m	$\delta$ (CH <sub>2</sub> )
1389 s		1387 w		
1377 sh	1388 m	1377 w	1382 m	$\omega$ (CH <sub>2</sub> )
1352 m	1340 sh	1346 w	1342 sh	t (CH <sub>2</sub> )
1330 (a)				
1320 sh				$\omega$ (CH <sub>2</sub> )
1310 s	1315 s	1309 s	1317 s	
1275 vs	1269 vs	1273 s	1273 m	$\nu_s$ (NO <sub>2</sub> )
1271 vs				
1234 m	1230 sh	1232 sh	1230 sh	$\nu$ (NN)
1219 m		1214 s	1216 m	
1040 s	(g)	1029 w	(g)	ring
1019 m	1020 w	1018 sh		
947 m	931 s	943 w	945 vvw	r (CH <sub>2</sub> )
926 s		920 w		ring
915 sh	917 sh			
883 m	885 w	884 vs	886 vs	ring and $\delta$ (NO <sub>2</sub> ) (f)
853 w	817 w	855 sh	856 sh	(NO <sub>2</sub> )
844 w		847 s	846 m	ring and $\delta$ (NO <sub>2</sub> ) (f)
783 s	791 vs	786 w	798 m	
755 m	766 m	756 vw	(g)	$\omega$ (NO <sub>2</sub> ) (d)
738 vw		739 vw		
670 vw	662 vw	669 w		
602 m	602 sh	605 m	606 m	r (NO <sub>2</sub> ) (d)
588 m	586 vw	589 m	592 m	
486 w	498 vw	486 w sh		ring
461 w	469 vw	463 m	472 s	

Table 6 (continued)

Infrared (cm <sup>-1</sup> )		Raman (cm <sup>-1</sup> )		Assignment
Solid	Solution	Solid	Solution	
		440 (b)		$\gamma$ (NN)
410 w	410 vw	414 m	410 w	and
345 vw	(g)	347 w	(g)	ring
300 (c)		301 (b)		
223 vw	218 (c)	224 s	220 s	$\delta$ (NN)
208 vw		205 m		ring and $\delta$ (NN)

vs - very strong, s - strong, m - medium, w - weak, vw - very weak, vvv - extremely weak, sh - shoulder.

a) observed in cooled sample only

b) observed in single crystal sample only

c) computer averaged

d) discussed in text

e) overtone or combination vibration

f) coupled vibration

g) solvent interference

h) region not explored

## II. EXPERIMENTAL

### A. Materials Used

RDX, free of HMX contamination, was supplied by Dr. Suryanarayana Bulusa at Picatinny Arsenal, Dover, New Jersey. The RDX melted at 203.5-204.5°C. Thymol used during this research project was reagent grade, supplied by Aldrich Chemical Company, Inc., Milwaukee, Wisconsin, and was not purified further.

### B. Raman Spectroscopy

#### 1. Instrumentation

Raman spectra were recorded on a Spex Model 1401 double monochromator spectrometer employing photon counting. The laser source was a Spectra-Physics Model 164 argon ion laser operating at a wavelength of 4880 Å with a power output of 0.6-1.2 watts. Monochromator slit widths were set at 150 microns. The 218, 314 and  $458 \text{ cm}^{-1}$  bands of carbon tetrachloride were used to calibrate the spectrometer. This system was interfaced with a Nicolet 1180 data acquisition system which significantly enhanced the signal to noise ratio through signal averaging multiple scans of the sample spectra.

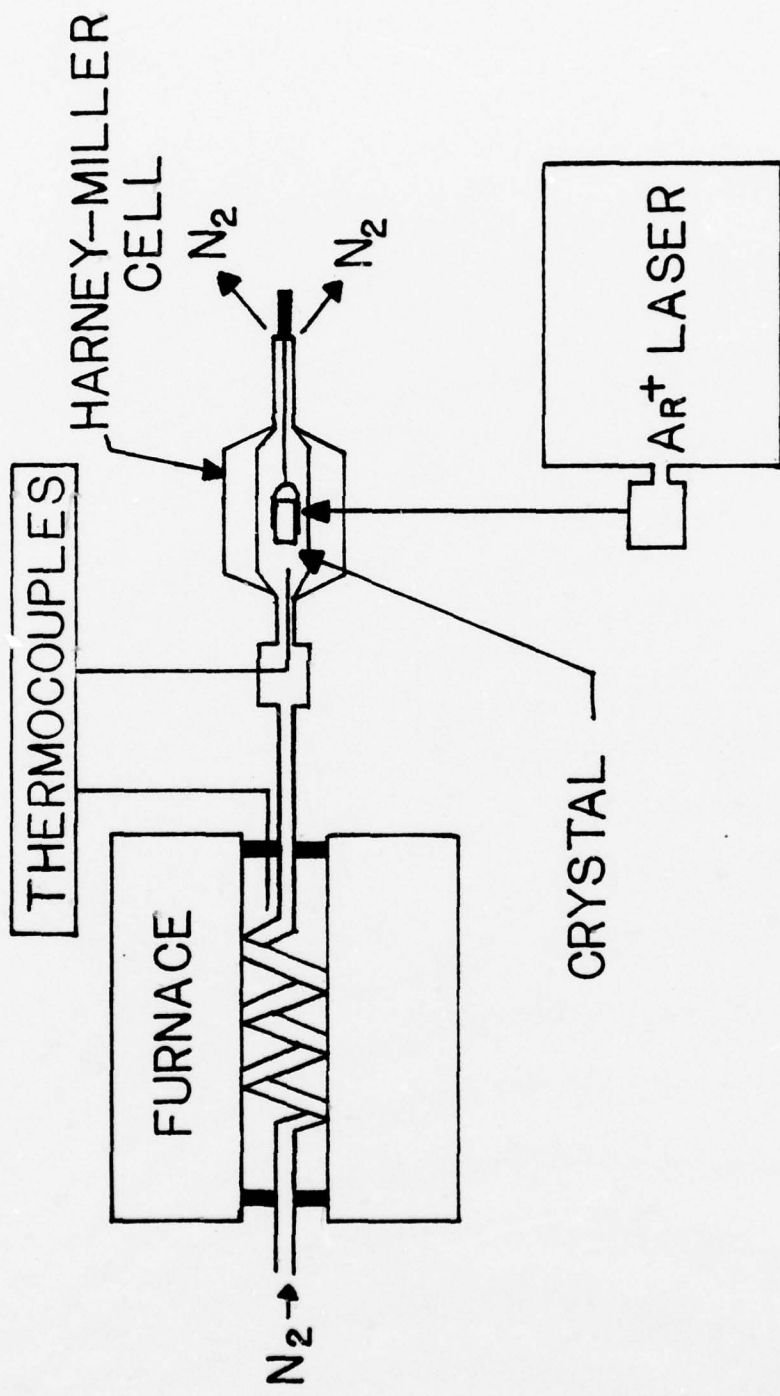
## 2. Dependence of Spectra on Sample Orientation

The first investigation conducted during this research project was an orientation study of a single crystal of RDX mounted on a eucentric goniometer. Single crystals were grown by slow evaporation of a RDX-saturated solution consisting of four parts acetone and one part water. Raman spectra were recorded over the frequency range  $40-1050 \text{ cm}^{-1}$ . Spectra were recorded for one complete revolution of the crystal at  $60^\circ$  increments. The single crystal was also suspended vertically and its spectrum recorded.

## 3. Slow Heating Experiments

Slow heating experiments were conducted employing the techniques and equipment developed by Brill and Goetz<sup>36</sup> and involved passing heated nitrogen gas over the sample. Figure 6 shows a block diagram of the system used. Both single crystals and powder samples were used during these investigations. Single crystals were mounted in glass capillary tubes having a thin-walled funnel-shaped end. These sample holding tubes were then mounted inside a Harney-Miller cell. Powder samples were contained in Kimax melting point capillary tubes, closed at one end, which were themselves placed inside the Harney-Miller cell. These tubes were filled to a height of 20-25 mm with RDX. Sample temperature was controlled by adjusting the nitrogen flow rate through a Pyrex heating coil placed in an electric tube furnace set at  $500^\circ\text{C}$ . A Fluke model 2100A digital thermometer with a Chromel-Alumel thermocouple positioned within 5 mm of the

Figure 6<sup>36</sup>  
Slow Heating Variable Temperature Cell Design



sample was used to monitor sample temperature. The sample was heated at a rate of 10°C per minute. Spectra were recorded in approximately 25°C intervals from room temperature to 180°C. Sample decomposition limited attempts to record spectra using slow heating techniques at temperatures in excess of 180°C. The system was calibrated previously<sup>5</sup> and checked regularly with hexachlorobenzene which was found to melt within  $\pm 1^{\circ}\text{C}$  of its literature melting temperature.<sup>37</sup> Spectra were recorded over the frequency range 40-1050  $\text{cm}^{-1}$  for several RDX samples at the various temperatures investigated. An average frequency for each band was determined and plotted as a function of temperature. All spectra were recorded with a laser power of 0.6 watts and a monochromator scan speed of 60  $\text{cm}^{-1}/\text{min}$ .

#### 4. Rapid Heating Experiments

Rapid heating experiments involved immersing a sample of RDX contained in a capillary tube into a heated oil bath for a specific period of time and then recording the sample spectrum. The oil bath consisted of Silicone fluid in a Pyrex crystallizing dish (199 mm x 10 mm) filled to a depth of 1-1/2 inches, heated and stirred on a Corning combination hotplate/magnetic stirrer. Oil temperature was monitored using a mercury thermometer. Samples were contained in a Kimax melting point capillary tube, closed at one end, and filled to a height of 20-25 mm. Sample tubes were attached to the side of the thermometer and heated at a rate of approximately 50°C/sec. All samples heated to 200°C or less were placed in the oil bath for 5 minutes to insure uniform temperature throughout the sample.

Samples heated to 203°C were placed in the oil bath for a maximum of 35 seconds because rapid sample decomposition occurs at this temperature. Samples heated to 210°C were placed in the oil bath for 15 seconds. After being removed from the oil bath, sample capillary tubes were wiped clean with an acetone moistened paper towel, placed in the sample compartment and their spectra recorded. Recording of spectra commenced within 30 seconds after samples were removed from the oil bath. Spectra were recorded first over the frequency range 40-200  $\text{cm}^{-1}$ . After changing electronic settings on the instrument to compensate for lower band intensities of the internal vibrational modes, the remaining region was then recorded in the frequency range of 200-1050  $\text{cm}^{-1}$ . Complete spectra were recorded for several RDX samples at each temperature selected. Additionally, spectra of selected individual bands were recorded for several RDX samples at each temperature. An average frequency for each band was then determined and plotted as a function of temperature. All spectra were recorded with a laser power of 1.2 watts and a monochromator scan speed of 50  $\text{cm}^{-1}/\text{min}$ .

##### 5. $\beta$ -RDX in Thymol

These experiments involved attempts at preparing the  $\beta$ -polymorph of RDX by recrystallizing a mixture of the two polymorphs from a supersaturated solution of RDX dissolved in molten thymol. A modification of the method described by McCrone<sup>3</sup> was used for these preparations. Spectra of the recrystallized RDX in thymol were then recorded. The polymorph mixture was prepared by heating 1.1 g

(7.32 mmol) of thymol in a 5 mL beaker to 150°C, on a Corning combination hotplate/magnetic stirrer, and stirring with a Teflon stirring bar. To the molten thymol was added either 40 mg (0.135 mmol) or 120 mg (0.540 mmol) of RDX with continued stirring for three minutes. When 120 mg of RDX was added, a saturated solution resulted and a small amount of undissolved RDX remained on the bottom of the beaker. These solutions were then rapidly cooled by being drawn into a capillary tube at room temperature, resulting in the recrystallization of a mixture of  $\alpha$ - and  $\beta$ -RDX. Temperature was monitored using a Chromel-Alumel thermocouple connected to a Fluke Model 2100A digital thermometer.

When cooled from 150°C to room temperature, molten thymol containing dissolved RDX existed as a supercooled liquid. However, if sufficiently disturbed, it readily nucleated and crystallized. A special handling procedure was therefore needed to accomplish transfer of the molten thymol solution from the reaction beaker to a capillary tube. Transfer of solution from the beaker to a capillary tube was accomplished using a Kimex melting point capillary tube, open at both ends, and a pipet suction bulb. The open end of the rubber bulb was sealed off with a Hoffman pinchcock clamp and a small hole was pierced in the opposite solid end. One end of the capillary tube was then inserted through the pierced hole in the rubber bulb resulting in a "micro pipet" into which was drawn a sample of the heated solution to a height of approximately 40 mm. RDX recrystallized out of the heated solution as a mixture of the

two polymorphs. The thymol remained as a supercooled liquid. The sample-containing end of the capillary tube was sealed off with a small piece of Parafilm and the sample spectrum was recorded over the frequency range  $40\text{-}1050\text{ cm}^{-1}$ .

Recording of the spectrum was initiated within 30 seconds after the solution was drawn into the capillary tube. Spectra were recorded for many samples prepared in different batches. In addition, spectra were recorded over the frequency range  $40\text{-}1050\text{ cm}^{-1}$  for pure RDX, which had been heated to  $150^{\circ}\text{C}$  and then cooled to room temperature, and for pure thymol in both the supercooled liquid state and in the crystalline form. All spectra were recorded with a laser power of 1.2 watts and a monochromator scan speed of  $50\text{ cm}^{-1}/\text{min}$ .

### C. Polarizing Microscope

Optical crystallographic properties of RDX<sup>2</sup> were examined, using a Leitz Model Orthoplan research polarizing microscope, for the purpose of identifying the  $\beta$ -polymorph. The  $\beta$ -polymorph was prepared by recrystallization from a supersaturated solution of RDX in molten thymol according to the procedure described above. Solution samples were transferred from the reaction beaker to room temperature microscope slides using a medicine dropper heated on the reaction hotplate to  $150^{\circ}\text{C}$  (solution temperature). This resulted in rapid cooling of the hot solution causing recrystallization of the two polymorphs. Room temperature cover slips were then placed

on top of the samples. Samples prepared from several different batches were examined.

An additional experiment was carried out to determine if the 4880 Å wavelength, 1.2 watt laser beam used in the Raman investigation was detrimental to the recrystallized needle shaped RDX crystals<sup>2,3</sup> observed under the polarizing microscope. A microscope slide with needle shaped crystals recrystallized on it was irradiated with the laser beam for 10 minutes and then studied again under the polarizing microscope to observe any changes.

#### D. X-Ray Diffraction Powder Patterns

Attempts were made to observe the  $\beta$ -polymorph of RDX by recording the X-ray powder pattern of RDX recrystallized from a super-saturated solution of RDX in molten thymol according to the procedure described above. A Philips Norelco vertical circle goniometer with a diffracted beam graphite monochromator was used in the X-ray diffraction powder pattern investigations. Cu,  $K_{\alpha}$  radiation was supplied by an X-ray tube operated at 35 kv and 20 ma. Samples were scanned from 60°-10° at a scan speed of 1°/min with signals being filtered electronically by a pulse height analyzer. Hot solution samples were carefully deposited on glass slides at room temperature using a heated medicine dropper. This resulted in recrystallization of a mixture of the two polymorphs. Thymol remained as a super-cooled liquid. Several powder patterns were recorded of RDX recrystallized from molten thymol prepared in different batches. Also,

X-ray powder patterns were recorded for pure crystalline  $\alpha$ -RDX and  
for pure crystalline thymol to aid in assigning the different lines.

### III. RESULTS AND DISCUSSION

#### A. Raman Spectroscopy

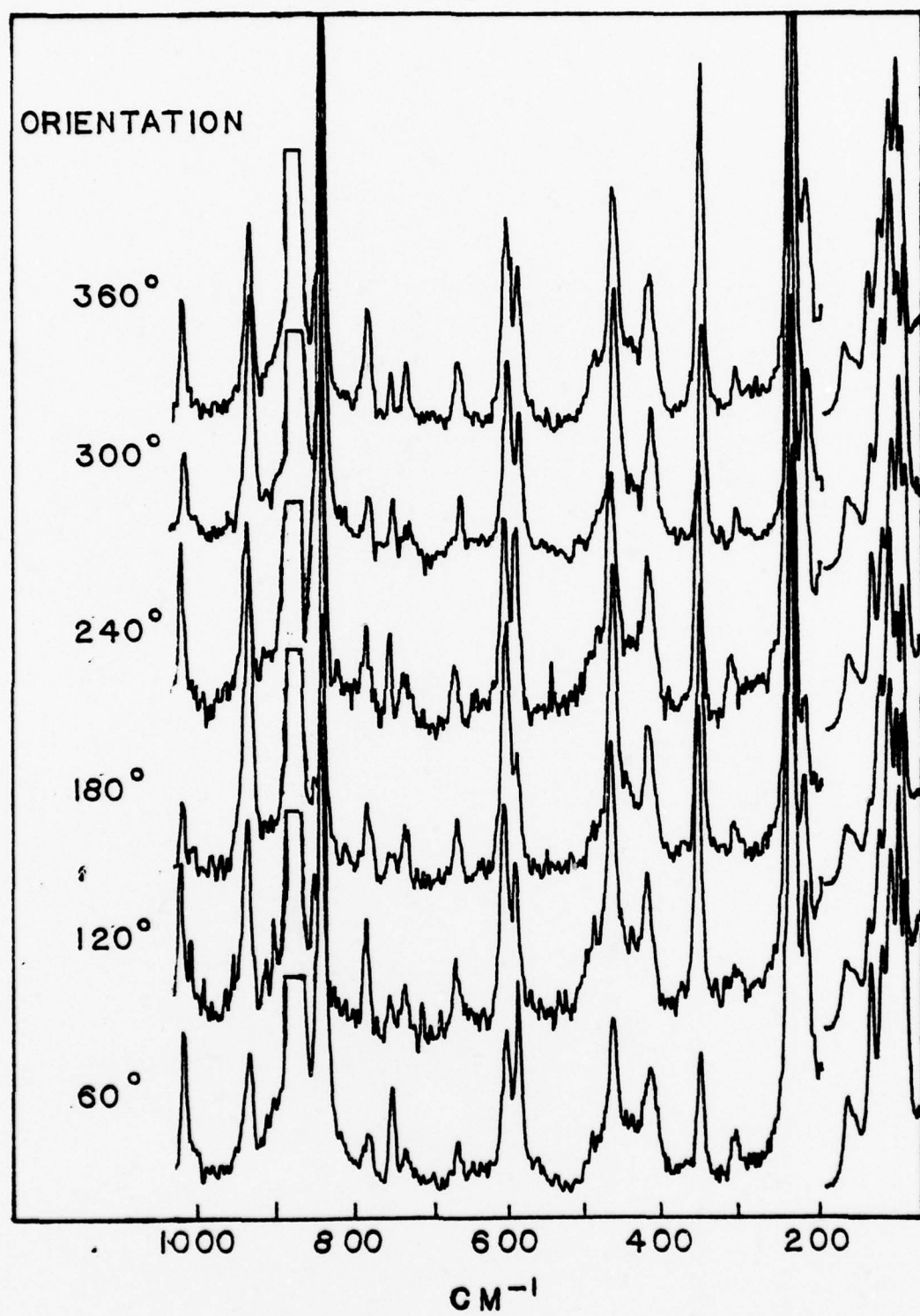
##### 1. Dependence of Spectra on Sample Orientation

Before investigating the spectra of RDX as a function of temperature, it was necessary to ascertain whether or not sample spectra were sensitive to crystal orientation. A single crystal of RDX was rotated through 360 degrees and multiple scans of its spectrum were recorded at room temperature after each 60 degrees of rotation. The initial crystal orientation designated as 360 degrees was chosen arbitrarily. The crystal was also suspended vertically and its spectrum recorded. Figure 7 shows the results of this investigation. The spectrum of the vertically suspended sample is not shown in Figure 7 because of extensive noise encountered in recording its spectrum. However, for the vertical orientation all bands of medium and strong intensity that could be distinguished from background noise were in agreement, in all respects, with bands recorded for the rotated crystal. As shown in Figure 7 marked variations in relative band intensities were observed, however, the number of bands and band widths remained constant. Band positions did not vary in frequency by more than  $\pm 1 \text{ cm}^{-1}$ . Thus, it was shown that the vibrational frequencies of

Figure 7

Raman Spectra of Single RDX Crystal

as a Function of Orientation



of RDX are not orientation dependent and this factor was discounted as controlling the position and number of bands observed in subsequent investigations of this compound.

## 2. Slow Heating Experiments

The vibrational spectrum of RDX at room temperature has been examined in several reports.<sup>32,33,34</sup> Additionally, the infrared spectrum of RDX as a function of temperature has been investigated.<sup>35</sup> A complete infrared and Raman analysis of RDX at room temperature has been reported by Iqbal, *et al.*,<sup>32</sup> and Rey-Lafon, *et al.*,<sup>33,34</sup> who carried out a <sup>15</sup>N isotope substitution study and determined the band assignments over the entire spectrum. However, no Raman investigations have been conducted which examined the effects of heating on RDX. Goetz and Brill<sup>5</sup> conducted a laser Raman investigation of HMX as a function of temperature and observed thermally induced polymorph interconversions as evidenced by a change in the number and position of bands recorded. Consequently, a temperature study of RDX was initiated in this project. Shown in Figure 8 is the room temperature spectrum of RDX with vibrational frequencies and assignments listed in Table 7. Slow heating experiments conducted on both crystals and powdered samples of RDX showed identical results. Samples were heated at a rate of 10°C/min and multiple scans of sample spectra were recorded at approximately 25°C intervals for both internal and external modes. Heating experiments were repeated several times to insure their reproducibility. At

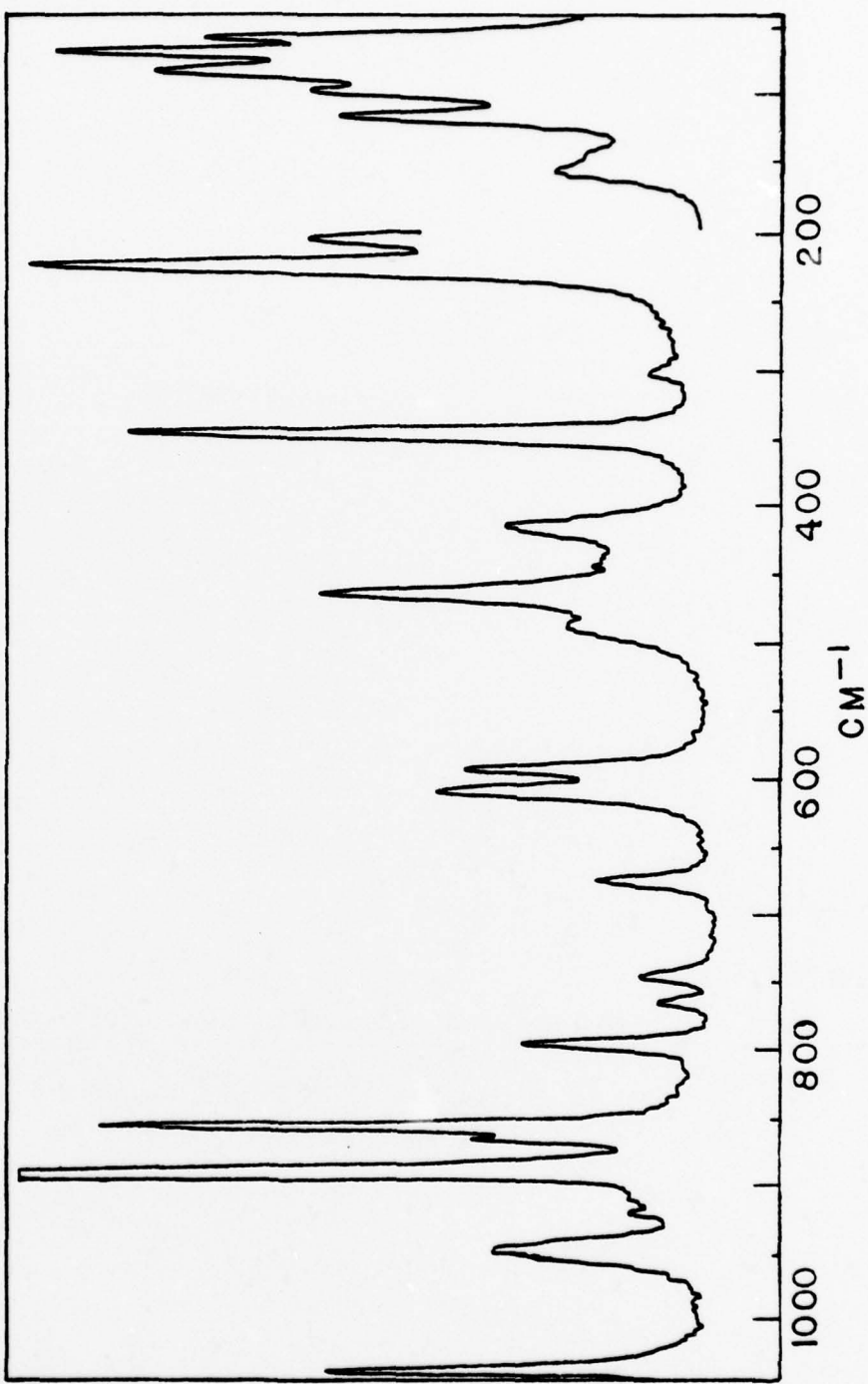


Figure 8  
Partial Raman Spectrum of RDX at Room Temperature

Table 7  
Frequencies ( $\text{cm}^{-1}$ ) and Assignment of Bands in RDX Spectrum

Frequency	Assignment $^{32}$	Frequency	Assignment $^{32}$
45 <sup>9</sup> <sup>a</sup>		670 w	
56 s		738 w	
69 s	Lattice modes	757 w	$\text{NO}_2$ deformation
87 m		787 m	
106 m		846 s	
129 w br		856 m sh	
149 m br	$\text{N-NO}_2$ torsion	883 vs	Symmetric ring stretch
206 m	C-N-C bend + torsion	921 w	
225 s		943 m	
301 w		1030 m	Ring
346 s	C-N-C bend		
414 m			
463 m			
486 w br	$\text{NO}_2$ skeletal		
591 m			
606 m			

a)  $\text{vs}$  - very strong,  $\text{s}$  - strong,  $\text{m}$  - medium,  $\text{w}$  - weak,  $\text{sh}$  - shoulder,  $\text{br}$  - broad

approximately 180°C and above sample decomposition and extensive noise rendered the recording of sample spectra virtually impossible. At these high temperatures, weak bands could not be distinguished from background noise. Also, powder samples contained in capillary tubes decomposed giving off gas bubbles which moved the sample along the length of the capillary tube and thus out of the laser beam. Examination of the spectra recorded during the slow heating experiments showed that no changes occurred in the number, position or width of bands recorded. Hence, it was concluded that slow heating of RDX up to a temperature of 180°C does not induce a phase transition.

### 3. Rapid Heating Experiments

As a compliment to the slow heating experiments and to verify their results, rapid heating experiments were conducted. In these investigations, powdered samples of RDX were heated at a rate of approximately 50°C/sec and their spectra were recorded as described in the experimental section. These experiments were repeated several times to insure their reproducibility. Samples heated to 203°C and 210°C were observed to melt and begin to decompose almost instantaneously after being immersed in the oil bath, however, they immediately solidified after being removed. Recording of spectra, even at the higher temperatures, produced sharp distinct bands with little of the associated noise found in the slow heating experiments. However, as in the slow heating investigations no changes were observed to occur in the number, position or width of bands recorded.

Thus, in contrast to the results obtained by Goetz and Brill<sup>5</sup> with heating experiments on HMX, it is concluded that neither rapid heating nor slow heating produce any solid phase transformations in RDX. Furthermore, McCrone reported that  $\beta$ -RDX was produced when  $\alpha$ -RDX was fused then cooled.<sup>2</sup> In the rapid heating experiments, RDX was fused when heated to 203°C and 210°C. It was cooled when the sample containing capillary tubes were removed from the hot oil bath. However, all bands in the spectra recorded for these samples were unequivocally assigned to the  $\alpha$ -polymorph.

#### 4. $\beta$ -RDX in Thymol

Having demonstrated in the previous experiments that the  $\beta$ -polymorph of RDX could not be produced and observed by heating of the  $\alpha$ -polymorph, a modification of the micro hot stage method described by McCrone<sup>2,3</sup> was employed to prepare the  $\beta$ -polymorph. Attempts were then made to record its spectrum. To aid in the assignment of bands, the spectrum was recorded for pure thymol heated to 150°C and then cooled to room temperature resulting in a supercooled liquid. Spectra were also recorded for pure crystalline thymol and for pure RDX heated to 150°C and cooled to room temperature. Figure 9 shows the spectra over the frequency range 40-1040  $\text{cm}^{-1}$  for the pure samples described above. Band frequencies are listed in Table 8. Examination of the spectra showed that many thymol bands and RDX bands overlapped, however, each sample exhibited some unique bands. When spectra were recorded for dilute

**Figure 9**

**Raman Spectra of Pure RDX, Crystalline  
Thymol and Liquid Thymol**

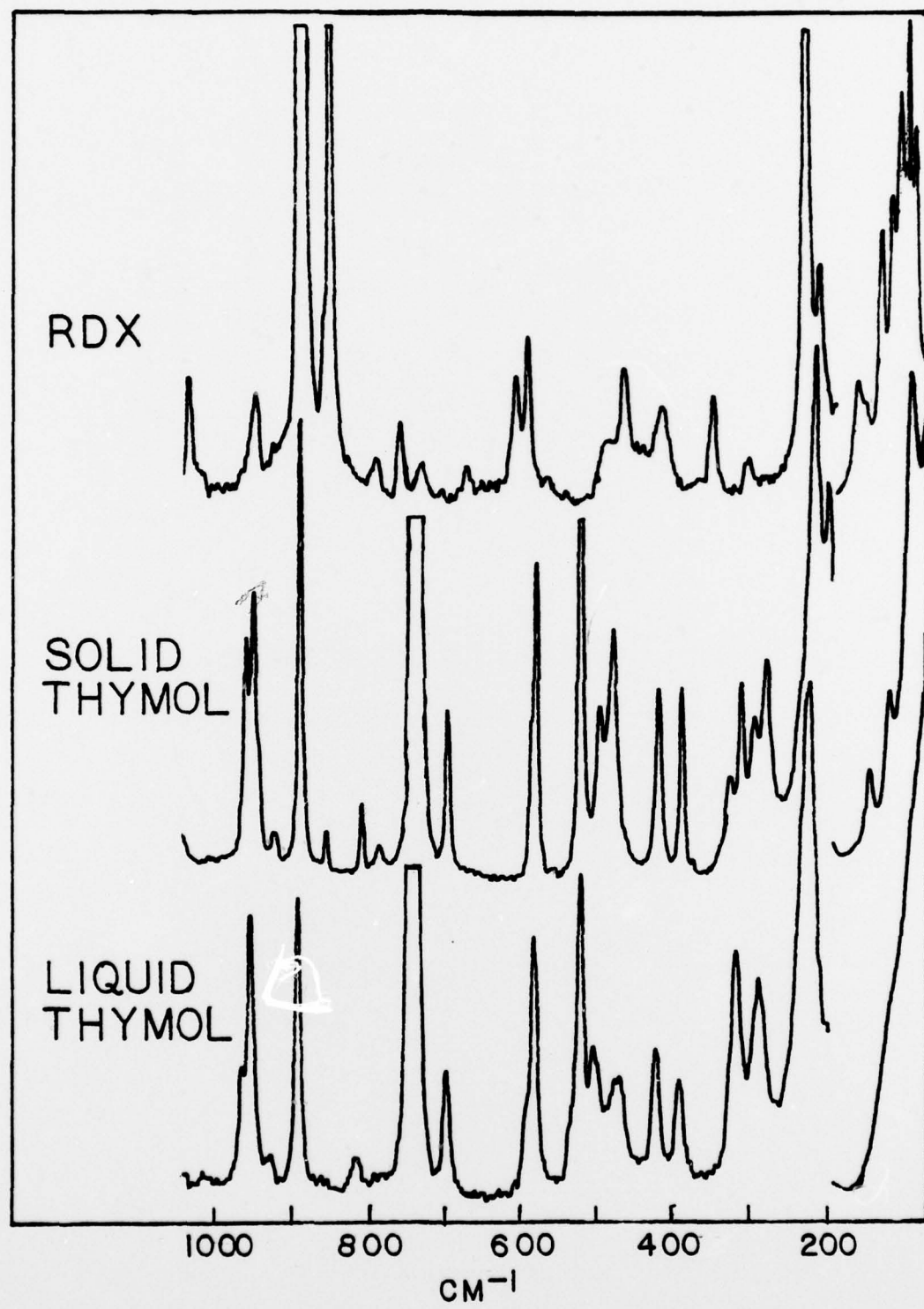


Table 8  
 Frequencies of Bands ( $\text{cm}^{-1}$ ) in Raman Spectrum of  
 Pure Thymol and Pure RDX

<u>Liquid Thymol</u>	<u>Crystalline Thymol</u>	<u><math>\alpha</math>-RDX</u>
		45
		56
	62	69
		87
	106	106
		129 w
	140	149
	205	206
226	223	225
289	284	
	301 w <sup>a</sup>	301 w
320	318	
	332 w	
		346
393	394	
424	424	414
470		463
	483	486 w
505	500 w	
520	524	
580	583	
	590 sh <sup>b</sup>	591
		606
		670 w
695	697	
737	738	738 w
		757 w
	786 w	787
810 w	808	
		846
	854 w	856 sh
884	885	883
921 w	919 w	921 w
945	946	943
956 w	955	
		1030

a) weak

b) shoulder

solutions of RDX recrystallized from molten thymol (40 mg of RDX in 1.1 g of thymol), the only unique RDX bands observed were at  $346\text{ cm}^{-1}$  and  $846\text{ cm}^{-1}$ . These are the two most intense bands of  $\alpha$ -RDX. All other bands recorded were attributed to the thymol.

Figure 10 shows the spectrum of a saturated solution of RDX recrystallized from molten thymol (120 mg of RDX in 1.1 g of thymol).

Band frequencies are listed in Table 9. Examination of Figure 10 revealed that even the most intense unique RDX bands were weak in comparison to the thymol bands. Thus, if  $\beta$ -RDX were present and exhibited only weak bands it could not be detected. All bands recorded for the recrystallized RDX in thymol were assigned to either  $\alpha$ -RDX or thymol. No new bands were observed and no frequency shifts occurred.

Two theories are offered to explain why  $\beta$ -RDX prepared in these experiments was not observed spectroscopically. First, it was reported by McCrone<sup>2,3</sup> that  $\beta$ -RDX is highly unstable and very rapidly converts to the  $\alpha$ -polymorph. During the time required to record its Raman spectrum, the  $\beta$ -polymorph could have completely converted to the  $\alpha$ -polymorph. Secondly, McCrone<sup>2,3</sup> reported that when RDX was recrystallized from molten thymol both the  $\alpha$ - and  $\beta$ -polymorphs were prepared. Examination of his microphotographs revealed that the  $\alpha$ -polymorph recrystallized predominantly with only a small concentration of the  $\beta$ -polymorph being present. Thus, as discussed above, unless the  $\beta$ -polymorph exhibited a very intense

Figure 10  
Raman Spectrum of Recrystallized RDX in Thymol

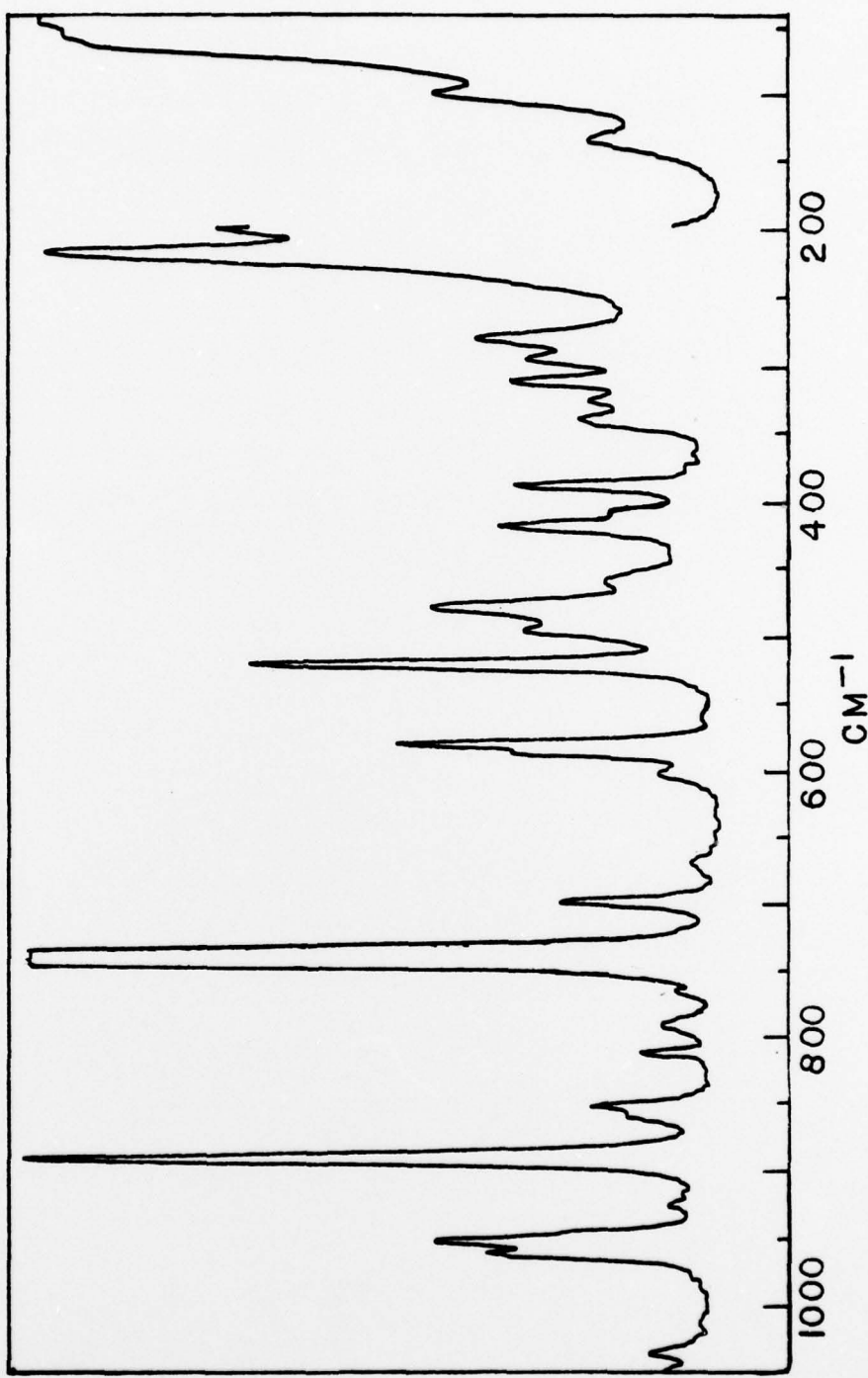


Table 9

Frequencies and Assignment of Bands in Raman Spectrum  
of RDX Recrystallized in Thymol

<u>Frequency</u>	<u>Assignment</u>	<u>Frequency</u>	<u>Assignment</u>
45 w <sup>a</sup>		525	T
55 w		583	T
67 sh, <sup>b</sup> w		590 sh	T + R
105		605 w	R
140		669 w	R
206	T <sup>c</sup> + R <sup>d</sup>	698	T
225	T + R	738	T + R
287	T	757 w	R
301	T + R	786 w	T + R
318	T	807 w	T
333	T	846	R
346	R	855 sh	T + R
394	T	883	T + R
414 sh	R	919 w	T + R
423	T	945	T + R
463	R	955	T
485	T + R	1029 w	R
500	T		

a) weak

b) shoulder

c) thymol

d)  $\alpha$ -RDX

unique band in its Raman spectrum, it would not be detected due to the intense  $\alpha$ -RDX and thymol bands.

B. Polarizing Microscope

A polarizing microscope was utilized to ascertain the existence of  $\beta$ -RDX when prepared according to a modification of the micro hot stage method described by McCrone. McCrone reported that both platelets of  $\alpha$ -RDX and fine dendritic crystals of  $\beta$ -RDX were produced when RDX was recrystallized by rapid cooling from a supersaturated solution of RDX in molten thymol.<sup>3</sup> The  $\beta$ -polymorph was then observed to dissolve as the  $\alpha$ -polymorph grew via a solution-phase transformation.<sup>3</sup>

RDX was recrystallized on a room temperature microscope slide by depositing a drop of solution consisting of 40 mg of RDX dissolved in 1.1 g of molten thymol on the slide. The thymol remained as a supercooled liquid. Examination of the recrystallized RDX under a polarizing microscope showed that both platelets and small fine needles of RDX were produced. The platelets were found to be optically negative and thus were identified as the  $\alpha$ -polymorph.<sup>2</sup> Only once were needles produced that were large enough to enable a determination of their optical sign. They were observed to be optically positive which identified them as the  $\beta$ -polymorph.<sup>2</sup> All other attempts to prepare  $\beta$ -RDX resulted in producing, in addition to optically negative platelets, fine needles too small to enable a determination of their optical sign using a polarizing microscope.

When RDX was recrystallized from a saturated solution of RDX dissolved in molten thymol (120 mg of RDX in 1.1 g of thymol), only agglomerates of needle shaped RDX crystals were produced. In all cases, the optical sign of the crystals in these agglomerates was found to be negative, indicating only the  $\alpha$ -polymorph was present.

An experiment was conducted to determine if the 4880  $\text{\AA}$  wavelength, 1.2 watt laser beam used during the Raman investigations might affect the  $\beta$ -RDX. In this experiment, RDX was recrystallized from a dilute solution of RDX dissolved in molten thymol prepared by the method described previously. Both platelets and fine needles of RDX were observed using a polarizing microscope. The microscope slide containing the two polymorphs was then placed in the path of the laser beam and allowed to remain there for 10 minutes. The laser beam was directed through a portion of the sample on the slide observed to contain the fine needle shaped crystals of  $\beta$ -RDX. After ten minutes had elapsed, the slide was removed from the laser beam and the sample was again observed under a polarizing microscope. The small fine needles of  $\beta$ -RDX remained unchanged. Thus it was concluded that the laser beam was not instrumental in converting the  $\beta$ -polymorph to the more stable  $\alpha$ -polymorph. Why the fine needles of  $\beta$ -RDX remained in that polymorphic form for such a long period of time without changing to the  $\alpha$ -polymorph is uncertain at this point. However, no definite half-time for the  $\beta$ -polymorph has been reported. McCrone described the lifetime of the  $\beta$ -polymorph

as; existing for only a "few seconds",<sup>2</sup>  $\beta$ -RDX "soon disappears",<sup>3</sup> and  $\beta$ -RDX "slowly" changes to the  $\alpha$ -polymorph.<sup>3</sup>

### C. X-Ray Diffraction Powder Patterns

In this set of experiments, an X-ray diffractometer was utilized in an attempt to observe  $\beta$ -RDX prepared by recrystallization from a supersaturated solution of RDX dissolved in molten thymol. The  $\beta$ -polymorph was prepared as described previously with rapid cooling of the hot solution accomplished by deposition on a glass slide at room temperature. X-Ray powder patterns were recorded for pure RDX and pure powdered thymol. Examination of these powder patterns showed that thymol exhibited a large number of lines, many of which overlapped RDX lines. To eliminate this problem, samples of RDX dissolved in molten thymol were very carefully deposited on the glass slides to insure that as the two RDX polymorphs recrystallized, the thymol remained as a supercooled liquid. All lines observed in the powder patterns of recrystallized RDX in liquid thymol were attributed to the  $\alpha$ -polymorph of RDX. As further evidence that none of the lines resulted from the unstable  $\beta$ -polymorph, immediately after recording the powder pattern of the recrystallized RDX sample, a second recording of its powder pattern was initiated. Fifty minutes were required to complete each recording. The two powder patterns were then compared to determine if any lines decreased in intensity as other lines grew.

No changes were observed. The number, intensity and spacing of all lines remained constant.

The above results are consistent with other findings of this research project. Two explanations are offered for why  $\beta$ -RDX was not observed. First, when prepared by recrystallization from RDX in molten thymol, the  $\alpha$ -polymorph predominates and a sufficient concentration of the  $\beta$ -polymorph is not produced to enable its X-ray powder pattern to be recorded. Secondly,  $\beta$ -RDX may convert to the  $\alpha$ -polymorph before its powder pattern can be recorded.

#### D. Conclusions

Three different methods were employed in attempts to prepare  $\beta$ -RDX during this research project. The  $\beta$ -polymorph could not be observed by either differential scanning calorimetry<sup>31</sup> or differential thermal analysis.<sup>20</sup> The only evidence for  $\beta$ -RDX continues to be the optical crystallographic properties noted by McCrone.<sup>2</sup>  $\beta$ -RDX could not be observed by Raman spectroscopy or X-ray powder diffraction, at least not by using the techniques employed here. The  $\beta$ -polymorph seems not to play a role in reactions of the heated material in the solid phase. No evidence was found for the existence of  $\beta$ -RDX in the presence of  $\alpha$ -RDX up to the melting point of the sample. The  $\beta$ -polymorph would appear to be mainly a research curiosity that is probably not particularly important to consider in modeling the molecular behavior of heated RDX. This fact is in

contrast to the polymorphs of HMX which appear to be important in the solid phase chemistry and physics of heated HMX.<sup>5,38</sup>

## BIBLIOGRAPHY

1. C. L. Coon and J. M. Guimont, U.S. NTIS. AD/A Rep. 1974, No. 005654/9GA, Standord Res. Inst., Menlo Park, CA.
2. W. C. McCrone, Analytical Chemistry, 22, 954 (1950).
3. W. C. McCrone, Microchem. J. Symp., Ser. 2, 243 (1962).
4. N. H. Hartshorne and A. Stuart, Crystals and the Polarizing Microscope, 4th ed., Edward Arnold Ltd., London, 1970, p. 483.
5. F. Goetz and T. B. Brill, J. Phys. Chem., submitted for publication.
6. S. Fordham, High Explosives and Propellants, Pergamon Press, N. Y., 1966, p. 37.
7. T. L. Davis, Chemistry of Powder and Explosives, John Wiley and Sons, Inc., New York, 1943, p. 396.
8. W. E. Bachmann and J. C. Sheehan, J. Am. Chem. Soc., 71, 1842 (1949).
9. K. Singh, J. Sci. Industr. Res., 15A, 450 (1956).
10. Y. P. Carignan and D. R. Satriana, J. Org. Chem., 32, 285 (1967).
11. J. Patterson, N. I. Shapira, J. Brown, W. Duckert, and J. Polson, EPA-600/2-76-2136, Oct. 1976, U.S. Environmental Protection Agency, Cincinnati, Ohio.
12. R. Hultgren, J. Chem. Phys., 4, 84 (1936).
13. P. M. Harris and P. T. Reed, AFOSR-TR-59-165, Ohio State University, 1959.
14. A. Filhol, Engineering Doctoral Thesis, University of Bordeaux, Talance, France, 1970.
15. C. S. Choi, Acta Cryst., B28, 2857 (1972).

16. A. Filhol, J. Phys. Chem., 75, 2056 (1971).
17. J. Stals, Aust. J. Chem., 22, 2505 (1969).
18. A. M. Soldate and R. M. Noyes, Analytical Chemistry, 19, 442 (1947).
19. A. R. Farminer and G. A. Webb, Tetrahedron, 31, 1521 (1975).
20. K. K. Miles, M.S. Thesis, Naval Postgraduate School, Monterey, California, 1972.
21. J. D. Cosgrove and A. J. Owen, Combustion and Flame, 22, 13 (1974).
22. F. C. Rauch and A. J. Fanelli, J. Phys. Chem., 73, 1604 (1969).
23. F. H. Pollard and R. M. H. Wyatt, Trans. Faraday Soc., 45, 760 (1949).
24. J. J. Batten, Aust. J. Chem., 24, 945 (1971).
25. J. D. Cosgrove and A. J. Owen, Combustion and Flame, 22, 19 (1974).
26. J. J. Batten, Aust. J. Chem., 24, 2025 (1971).
27. B. Suryanarayana, R. J. Graybush, and J. R. Autera, Chemistry and Industry, 2177 (1967).
28. J. J. Batten and D. C. Murdie, Aust. J. Chem., 23, 737 (1970).
29. A. J. B. Robertson, Trans. Faraday Soc., 45, 85 (1949).
30. J. J. Batten and D. C. Murdie, Aust. J. Chem., 23, 749 (1970).
31. P. G. Hall, Trans. Farady Soc., 67, 556 (1971).
32. Z. Iqbal, K. Suryanarayanan, S. Bulusa, and J. R. Autera, U.S. NTIS. AD Rep. 1972, No. 752899, Picatinny Arsenal, Dover, New Jersey.
33. M. Rey-Lafon, C. Trinquecoste, R. Cavagnat, and M. T. Forel, J. de Chemie Physique et de Physico-Chemie Biologique, 68(10), 1533 (1971).
34. M. Rey-Lafon, R. Cavagnat, C. Trinquecoste, and M. T. Forel, J. de Chemie Physique et de Physico-Chemie Biologique, 68(11-12), 1573 (1971).

35. A. Werbin, U.S. Atomic Energy Comm., UCRL-5078 (University of California, Livermore), 1957.
36. T. B. Brill and F. Goetz, AIAA Paper No. 76-205, 14th Aero-space Science Meeting, January 1976, Washington, D.C.
37. R. C. Weast, ed., Handbook of Chemistry and Physics, 56th ed., CRC Press, Cleveland, 1976, p. C-159.
38. F. Goetz, T. B. Brill, J. R. Ferraro, and L. J. Basile, to be published.